similar to those found in this work for the chelated vanadyl complexes VO(TCDA) and VO(DOCDA).

In summary, the analysis of the observed reactivity between VO(TCDA) or VO(DOCDA) and $[Ni([9]aneN_3)_2]^{3+}$ gives a consistent picture assuming the outer-sphere electron-transfer step to be rate-determining. The hydrolysis of the generated VOL species to the *cis*-dioxovanadium(V) complexes, which involves the unbinding of one coordinated pendant arm of the macrocyclic ligand, is a rapid subsequent step in reactions 8 and 9.

Acknowledgment. We thank the Fonds der Chemischen Industrie for financial support of this work. A.N. is grateful to CNPq (Brasil) for a stipend in 1987.

Registry No. **1**, 114675-42-2; **2**, 114675-44-4; VO(DOCDA), 114675-43-3; $[VO(TCDA)]^+$, 114691-60-0; $[VO(DOCDA)]^+$, 114675-45-5; $[Ni([9]aneN_3)_2]^{3+}$, 86709-81-1; $Li_2(TCDA)$, 114691-59-7; $Li_2(DOCDA)$, 114675-41-1; $VO(acac)_2$, 3153-26-2; 1,4,7-triazacyclononane, 4730-54-5; 2-bromoacetic acid ethyl ester, 105-36-2; 1-oxa-4,7-diazacyclononane, 80289-59-4.

Supplementary Material Available: Tables of refined and calculated positions of hydrogen atoms, anisotropic thermal parameters, and intraligand bond distances and angles for $[VO(TCDA)]\cdot H_2O$ and $[VO_2(TCDAH)]\cdot 2H_2O$ and a view of the second molecule in $[VO_2(TCDAH)]\cdot H_2O$ (8 pages); listings of observed and calculated structure factors (49 pages). Ordering information is given on any current masthead page.

Contribution from the Department of Chemistry, Brandeis University, Waltham, Massachusetts 02254

Kinetics and Mechanism of H_2O_2 Decomposition Catalyzed by Cu^{2+} in Alkaline Solution[1]

Yin Luo, Kenneth Kustin,* and Irving R. Epstein*

Received January 20, 1988

The kinetics of the Cu^{2+}-catalyzed decomposition of hydrogen peroxide have been studied at pH 11-12. The disappearance of hydrogen peroxide and the appearance of dissolved dioxygen have been followed titrimetrically and potentiometrically. Alkaline decomposition in the presence of copper(II) is accompanied by formation of a superoxide-copper(I) complex, formally, $[HO_2-Cu(I)]$. The apparent complex formation constant $K_{app} = [HO_2-Cu(I)]/[H_2O]_f[Cu^{2+}]_f$, where $[H_2O_2]_f$ and $[Cu^{2+}]_f$ are the concentrations of free hydrogen peroxide and free copper(II) ion, respectively, has been determined at several pH values. The results are consistent with a complex of molecular formula $HO_2Cu(OH)_2^-$, which has extinction coefficient $\geq 1600\ M^{-1}\ cm^{-1}$ at 345 nm and acid dissociation constant $K_c = [O_2Cu(OH)_2^{2-}][H^+]/[HO_2Cu(OH)_2^-] = 3.55 \times 10^{-12}$ M. The experimental time course of the reaction (graphs of $[H_2O_2]$ vs time) can be obtained by integrating the rate law $-dy/dt = wy^2/(v + sy + uy^2)$, where y is $[H_2O_2]$ and w, v, s, and u are complicated constants composed of rate constants and initial concentrations. Computer simulations with a mechanism in which complex formation is accompanied by reactions involving $OH^\bullet$, $HO_2^\bullet$, and $O_2^{\bullet-}$ radicals give excellent agreement with a variety of experimental observations. The relevance of the proposed mechanism to the Cu^{2+}-catalyzed decomposition of H_2O_2 in acid solution and to the Fe^{3+}-catalyzed reaction is discussed briefly.

Introduction

It has been known for about a century that the decomposition of H_2O_2 to H_2O and O_2 is drastically accelerated by many metal ions, among which Fe^{3+}/Fe^{2+} and Cu^{2+} have been investigated in depth.[2-6] Disagreements over mechanistic details, especially involving intermediate radicals or complexes, have lasted for decades.[7] There is evidence that the kinetics and mechanism of H_2O_2 decomposition catalyzed by iron and copper ions are dissimilar. This work focuses on the catalyst Cu^{2+}.

Sigel and colleagues[6] studied the kinetics of this reaction in acidic solution. A mechanism involving complexes but no radicals was suggested, which accounts for the experimental rate law. It assumes that, rather than changing its oxidation state, Cu^{2+} plays the role of a catalytic template that forms a bridge linking the two molecules of H_2O_2 that are going through oxidation and reduction.

Glasner[5] investigated the same reaction in alkaline solution with organic ligand present. He confirmed the formation of copper peroxide complex and used its absorbance to follow the reaction spectrophotometrically. Oxygen evolution out of the reaction solution was also measured. Both monitoring methods showed initial lags and fast subsequent increases in the reaction rate. Again, no radical was involved in the suggested mechanism.

However, the EPR experiment by Vierke[8] convincingly demonstrated the existence of $O_2^{\bullet-}$ and $OH^\bullet$ radicals in the decomposition of H_2O_2 catalyzed by Cu^{2+} at pH 12-13 in aqueous solution without organic ligands. Vierke further showed that when copper ion forms a complex (brown precipitate under his experimental conditions) with peroxide at the beginning of O_2 evolution, the EPR signal of copper(II) disappears. A new Cu(II) EPR signal, different from that of Cu^{2+}, CuO, or $Cu(OH)_2$, was detected after O_2 started to bubble and disappeared at the cessation of the bubbling. The molecular formula of neither the Cu(II) EPR-silent compound nor the EPR-active compound was identified.

We report here experiments carried out in strongly alkaline medium. We suggest a molecular formula for the Cu(II) EPR-silent copper peroxide complex, and we have measured its minimum extinction coefficient, as well as its equilibrium formation constant as a function of pH. We have determined the rate law valid in strongly alkaline solution and proposed a mechanism consistent with the experimentally observed rate law. We have fitted the integrated theoretical rates to the reaction progress curves

(1) Systematic Design of Chemical Oscillators. 44. Part 43: Citri, O.; Epstein, I. R. *J. Phys. Chem.* **1988**, *92*, 1865.
(2) Haber, F.; Weiss, J. *Proc. R. Soc. London, A* **1934**, *147*, 332.
(3) Barb, W. G.; Baxendale, J. H.; George, P.; Hargrave, K. R. *Trans. Faraday Soc.* **1951**, *47*, 462, 591.
(4) Kremer, M. L.; Stein, G. *Trans. Faraday Soc.* **1959**, *55*, 959.
(5) Glasner, A. *J. Chem. Soc.* **1951**, 904.
(6) Sigel, H.; Hierl, C.; Griesser, R. *J. Am. Chem. Soc.* **1969**, *91*, 106.
(7) Kremer, M. L. *Int. J. Chem. Kinet.* **1985**, *17*, 1299.
(8) Vierke, G. *Z. Naturforsch, B: Anorg. Chem., Org. Chem.* **1974**, *29B*, 135.

0020-1669/88/1327-2489$01.50/0

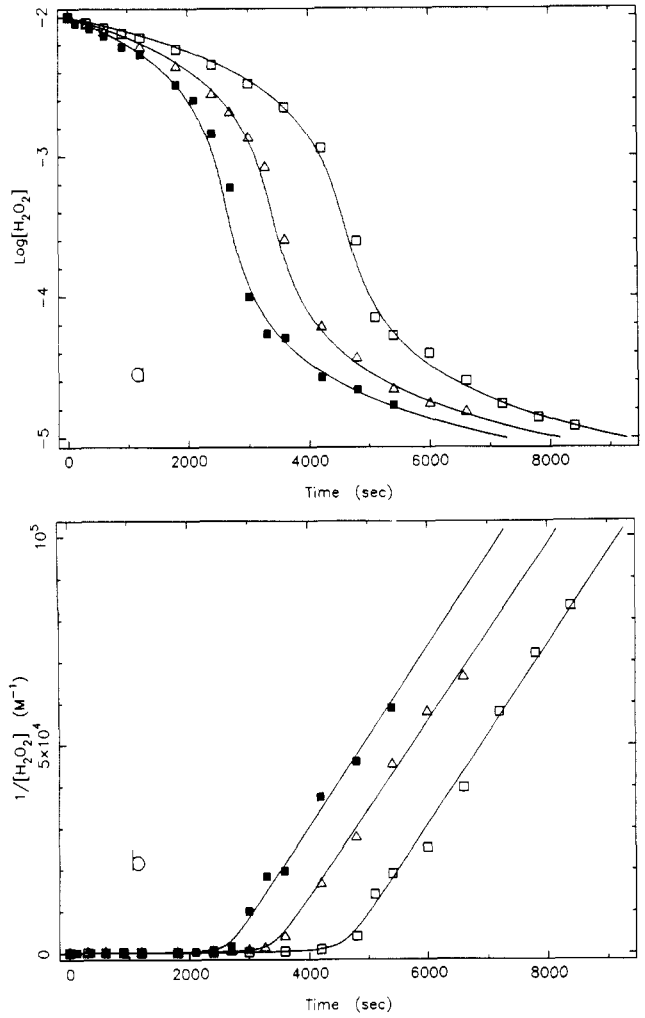

Figure 1. (a) Logarithm and (b) reciprocal of titrated H_2O_2 concentration vs time. Initial concentrations: $[H_2O_2]_0 = 1.0 \times 10^{-2}$ M; $[CuSO_4]_0 = 1.0 \times 10^{-4}$ M; $[NaOH]_0 = 1.0 \times 10^{-3}$ M (□), 3.0×10^{-3} M (△), 8.0×10^{-3} M (■). Solid lines are calculated correspondences determined by using eq 18 with parameters obtained from the nonlinear regression.

to estimate the unknown reaction rate constants in the mechanism.

Experimental Section

Materials. All chemicals were of the highest purity commercially available. Stock solutions of H_2O_2 were made weekly by diluting the 30% solution and were standardized daily with $KMnO_4$. It was found that the natural decomposition rate of 1 M aqueous H_2O_2 solution is about 1% in 24 h.

Methods. Any experiments that were not in thermostated instruments were performed at room temperature, about 20 °C. No attempt was made to regulate the ionic strength.

Titrimetric Experiments. The decomposition of H_2O_2 catalyzed by Cu(II) under both strongly acidic and strongly alkaline conditions can be monitored by sampling at intervals and titrating the unreacted H_2O_2 with standard $KMnO_4$ solution. The reaction in acid solution is much slower than the alkaline decomposition, being less than 10% complete after 24 h at pH 5.5, but it is 99% complete in less than 1 h at pH 11.0 with the same initial $[H_2O_2]$ and $[Cu^{2+}]$. This fact makes titrimetric measurements practical for the reaction in alkaline solution. Acidification effectively halts the more rapid alkaline decomposition at the desired time, and titrations with permanganate in acidic media can be carried out as much as 30 min later without significant discrepancy. The rate of hydrogen peroxide decomposition in alkaline solution was investigated at three different pH's with this method, and the results are shown in Figure 1.

O_2-Electrode Potentiometric Experiments. A Clark-type polarographic O_2 electrode (Hansa-tech DW-1) was employed to monitor the oxygen evolution at reaction initiation. The device was calibrated with air-saturated distilled water. All solutions were purged with N_2 for 30 min before being introduced into the reactor. The concentration of dissolved O_2 was thus reduced to about 6×10^{-5} M. A magnetic stirrer and the electrode membranes were at the bottom of the reaction vessel, which was

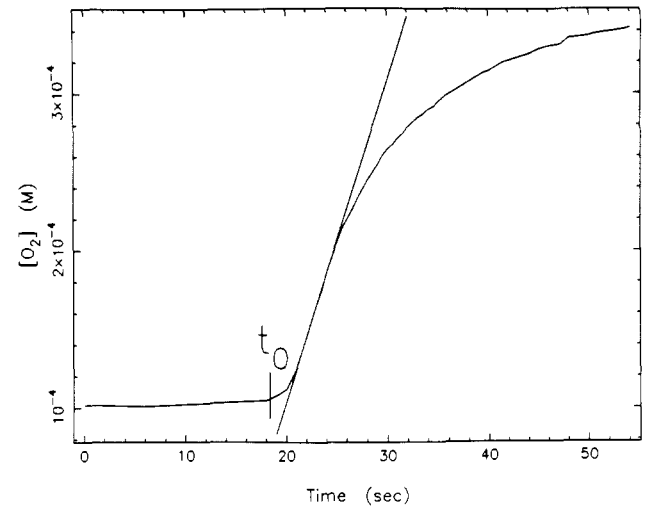

Figure 2. $[O_2]$ measured with the oxygen electrode. Initial concentrations: $[H_2O_2]_0 = 6.31 \times 10^{-4}$ M, $[CuSO_4]_0 = 1.0 \times 10^{-4}$ M, $[NaOH]_0 = 8.0 \times 10^{-3}$ M. $CuSO_4$ is injected at point t_0. The slope of the straight line yields the initial reaction rate (see text).

surrounded by a water jacket connected to a thermostated reservoir maintained at 26.0 ± 0.2 °C. The reactor was filled to a volume of about 1 mL with H_2O_2 and NaOH at the desired concentrations. After the base line was stabilized for at least 30 s, which is comparable to the measuring period of the reaction, the fast decomposition was initiated by injection of $CuSO_4$. The injection volume was 1% of the total volume.

An experimental trace is shown in Figure 2. In this particular experiment, $[H_2O_2]_0$ is relatively low, so that the total O_2 produced never exceeds the solubility and the oxygen-electrode potentiometry provides a profile of the entire reaction. In most of our measurements, we were able to follow only the initial portion of the reaction by this technique before the solution became saturated with O_2. The slope of the tangent after 1–2 s of mixing (maximum slope in the case of Figure 2) provides a measurement of the initial reaction rate. Replicate runs were done at each point, and reproducibility was satisfactory. By varying the initial concentration of each component, this method can be used to determine the initial rate law. Two concentration limits should be mentioned. The residual O_2 in the reagent solutions after N_2 purging sets the overall sensitivity of the instrument, which requires the initial concentration of H_2O_2 to be not lower than 10^{-4} M. Secondly, the fastest recording speed limits the pH to be ≤13.4.

Spectrophotometric Experiments. An absorbance spectrum (Perkin-Elmer 552A) was taken of the yellow solution that forms instantly when the pH of a solution of H_2O_2 and $CuSO_4$ is adjusted above 9. The absorbance peak partially overlaps with the broad H_2O_2 band below about 300 nm. Repetitive scanning over the duration of the reaction showed that the H_2O_2 absorbance decreases while the peak of the non-overlapped copper peroxide complex increases slightly in the first 10 min and then remains essentially constant until all H_2O_2 is consumed. The best wavelength for monitoring the complex was found to be 345 nm, though it may not be the absorbance maximum.

A reactor of volume 40 mL with quartz windows and thermostated at 25.0 ± 0.2 °C was built into the spectrophotometer. A magnetic stirrer at the bottom kept the solution homogeneous. The path length was 4.7 cm. Highly accurate calibration of the spectrophotometric cell was not necessary due to larger uncertainties described below. After establishment of the base line with H_2O_2 and NaOH, injection of $CuSO_4$ (1% of total reactor volume) triggered a fast rise in absorbance at 345 nm.

A lower limit on the extinction coefficient of the copper peroxide complex was estimated as 1600 M^{-1} cm^{-1} at 345 nm with a solution of H_2O_2 (10^{-2} M) + $CuSO_4$ (10^{-4} M) at pH 11–12. The chromophore concentration was taken to be the same as the initial $[Cu^{2+}]$, based on the expectation of a large equilibrium formation constant. Since, however, the complex is unstable[9,10] and decomposes soon after formation (see next section), the concentration of complex was overestimated, leading to an underestimate of the extinction coefficient. Measurements outside the above pH range were much less reliable and showed much larger standard deviations, because both the formation and decomposition are

(9) Aldridge, J.; Applebey, M. P. *J. Chem. Soc.* **1922**, *121*, 238.
(10) Teletov, I. S.; Veleshinetz, A. D. *Chem. Abstr.* **1930**, *24*, 5248; **1931**, *25*, 5635.

extremely rapid above pH 12 and because the formation is too slow relative to the decomposition below pH 11. In both cases we failed to detect the maximum in absorbance either because it took place before the reaction chamber was covered or because the peak never occurred.

Results and Mechanism

Qualitative Experiments. A number of qualitative experiments were performed to examine the effects of different chelating agents on the extent of catalyzed decomposition, which reveals the coordinational feature of the catalysis by copper ion. For example, a solution of 0.03 M H_2O_2, 0.002 M $CuSO_4$, and 0.01 M NaOH was made in a flask. Parallel experiments were carried on in the presence of sodium citrate and EDTA. The ratio of the concentration of organic ligand to that of Cu(II) was varied from 1:1 to 16:1.

Reaction in the presence of sodium citrate with [citrate]:[$CuSO_4$] = 4:1 closely resembles the reaction reported by Glasner:[5] the color changes sharply from light blue to intense yellow after a short quiescent period, and the burst of O_2 bubbles coincides with the appearance of the yellow color. Adding more sodium citrate, e.g., [citrate]:[$CuSO_4$] = 8:1 and 16:1, extended the lag period to 40 min and infinity, respectively. Titration of H_2O_2 with $KMnO_4$ after 20 h showed that 83% of the initial H_2O_2 decomposed in the 4:1 solution but less than 1% decomposed in the 16:1 solution. Reaction in the presence of the sodium salt of ethylenediaminetetraacetic acid with [EDTA]:[$CuSO_4$] = 1:1 gives results similar to those for [citrate]:[$CuSO_4$] = 4:1. Higher concentrations of EDTA suppressed the formation of yellow complex and the decomposition of H_2O_2.

As Glasner reported, however, the order of addition is important. The above observations were made with H_2O_2 as the last component added. If $CuSO_4$ is added last, the complex forms and O_2 evolves no matter what the value of the ratio [EDTA]:[$CuSO_4$]. However, the higher the ratio, the shorter the period before the color turns back to bright blue and O_2 bubbling halts. This observation implies that the formation constant for the copper–EDTA complex is larger than that for the copper–peroxide complex but that kinetically the rates of formation of the two complexes are in the opposite order or are of the same order of magnitude.

Formula of the Complex. The differences in rate law and color for solutions with the same formal concentrations of copper and hydrogen peroxide but different pH are indicative of different mechanisms of catalytic decomposition in acidic and alkaline media. It has been suggested[5] that the observed yellow complex of copper and peroxide is an essential intermediate in the alkaline catalysis. The above-mentioned experiments with organic ligands add further evidence for the complex's formation and for its being a key species in the catalyzed decomposition of H_2O_2.

Several studies[5,9-11] have attempted to assign a molecular formula to the copper peroxide complex. Wieland and Stein[11] suggest the formula $HO_2{\cdot}Cu{\cdot}O_2{\cdot}Cu{\cdot}O_2H$ based on study of the precipitates obtained at low temperature and with high concentrations of $CuSO_4$. Under our experimental conditions, however, there was no observable precipitate from the clear yellow solution before the cessation of O_2 bubbling.

As pointed out by Glasner,[5] Wieland and Stein did not determine the molecular weight, so that a monomer, e.g., $CuO{\cdot}O_2H$, may represent the compound as well. Most consistent with our studies is a monomer with a structure that can account for the high extinction coefficient, Cu(II) EPR silence, and a $CuO:H_2O_2$ ratio greater than unity[9,10] in basic solution, namely

$$HO_2Cu(OH)_n^{(n-1)-} \leftrightarrow O_2Cu(OH)_n^{n-} + H^+ \quad K_e \qquad (1)$$

The determination of n as 2 for the species in solution will be described later in this section.

The magnitude of the measured extinction coefficient certainly indicates an electron-transfer complex. In the molecules in eq 1, a one-electron transfer from hydrogen peroxide anion ligand to Cu(II) gives this feature. No Cu(II) EPR signal should be observable if electron transfer takes place, and the copper can be viewed as Cu(I) in coordination with superoxide. Further, if we assume that n in eq 1 is some number other than 1 for the solution but is essentially 1 for the precipitate, the equilibrium shown in eq 1 is consistent with the experimental analysis of the precipitate, $CuO:H_2O_2 > 1$.[9,10]

Under the assumption that $Cu(OH)_3^-$ and $Cu(OH)_4^{2-}$ are the only nonnegligible species of copper hydroxide in the pH range 11–12,[12] the following equilibria are proposed:

$$H_2O_2 + OH^- \leftrightarrow HO_2^- + H_2O \quad K_1 \text{ (M1)}$$

$$Cu^{2+} + HO_2^- + (n+1)OH^- \leftrightarrow O_2Cu(OH)_n^{n-} + H_2O \quad K_2 \text{ (M2)}$$

$$Cu^{2+} + H_2O_2 + (n+1)OH^- \leftrightarrow HO_2Cu(OH)_n^{(n-1)-} + H_2O \quad K_3 \text{ (M3)} \qquad (2)$$

$$Cu^{2+} + 3OH^- \leftrightarrow Cu(OH)_3^- \quad K_4 \text{ (M4)}$$

$$Cu^{2+} + 4OH^- \leftrightarrow Cu(OH)_4^{2-} \quad K_5 \text{ (M5)}$$

The known equilibrium constants are listed in Table I. (Note that the hydrolysis constants of copper, K_4 and K_5, are taken as the maximum values.[12])

The concentrations of all complexes can be calculated from the total initial concentrations, $[Cu^{2+}]_0$ and $[H_2O_2]_0$, the measured pH, and the equilibrium constants for reactions M1–5. The acidic and basic forms of the copper–peroxide complex, of H_2O_2, and of the couple $Cu(OH)_3^-/Cu(OH)_4^{2-}$ are kinetically indistinguishable. Consequently, the total concentration of copper peroxide complex, [HO_2–Cu(I)], and the total concentration of free hydrogen peroxide in solution, $[H_2O_2]_f$, are used to describe the system. Similarly, the total concentration of copper hydroxides is represented as $[Cu(OH)_x]$. The following relations are therefore valid when the rapid equilibria are established in the system:

$$[H_2O_2] = [H_2O_2]_f/(1 + K_1[OH^-]) = \alpha_1[H_2O_2]_f \qquad (3a)$$

$$[HO_2^-] = [H_2O_2]_f K_1[OH^-]/(1 + K_1[OH^-]) = \alpha_2[H_2O_2]_f \qquad (3b)$$

$$[HO_2\text{–Cu(I)}] = [HO_2Cu(OH)_n^{(n-1)-}] + [O_2Cu(OH)_n^{n-}] = (K_1K_2[OH^-]^{n+2} + K_3[OH^-]^{n+1})[H_2O_2]_f[Cu^{2+}]_f/(1 + K_1[OH^-]) = K_{app}[H_2O_2]_f[Cu^{2+}]_f \qquad (4)$$

$$[Cu(OH)_x] = [Cu(OH)_3^-] + [Cu(OH)_4^{2-}] = (K_4 + K_5[OH^-])[OH^-]^3[Cu^{2+}]_f \qquad (5)$$

where K_{app} represents the apparent formation constant of the complex and $[Cu^{2+}]_f$ is the concentration of free copper in solution that is in equilibrium with all other copper ions bound in complexes. Substitution of total initial [copper(II)] into eq 4 and 5 according to the relation

$$[Cu^{2+}]_f = [Cu^{2+}]_0 - [HO_2\text{–Cu(I)}] - [Cu(OH)_x]$$

and estimation of the free hydrogen peroxide in solution at early times as the initial or input concentration (since $[H_2O_2]_0$ is always

Table I. Equilibrium and Rate Constants

K, k		ref
K_1	2.4×10^2	
K_2	$<4.8 \times 10^{17}$ M^{-4}	this work
K_3	$<3.3 \times 10^{17}$ M^{-4}	this work
K_4	$<1.6 \times 10^{14}$ M^{-3}	12
K_5	$<2.5 \times 10^{16}$ M^{-4}	12
k_6	2.54×10^{-2} s^{-1}	this work
k_6'	6.93×10^{-3} s^{-1}	this work
k_7	$3–3 \times 10^9$ M^{-2} s^{-1}	this work
k_8	$5 \times 10–5 \times 10^9$ M^{-1} s^{-1}	this work
k_9	1.02×10^9 M^{-1} s^{-1}	18
k_{10}	see text	16

(11) Wieland, H.; Stein, E. *Z. Anorg. Allg. Chem.* **1938**, *236*, 361.

(12) Baes, C. F., Jr.; Mesmer, R. E. In *The Hydrolysis of Cations*; Wiley: New York, 1976; p 268.

Table II. Results of Linear Fits to the Experimental Data of the $1/A$ vs $1/[H_2O_2]_0$ Plots[a]

$[OH^-]$, M	intercept	slope	corr coeff	K_{app}
1.0×10^{-3}	1.43 ± 0.01	$6.26 \times 10^{-4} \pm 2.6 \times 10^{-5}$	0.995	4.18×10^{8}
2.5×10^{-3}	2.67 ± 0.06	$1.19 \times 10^{-3} \pm 6.1 \times 10^{-5}$	0.994	8.62×10^{8}
5.0×10^{-3}	1.35 ± 0.02	$5.70 \times 10^{-4} \pm 3.3 \times 10^{-5}$	0.992	8.43×10^{10}
1.0×10^{-2}	1.43 ± 0.01	$9.81 \times 10^{-4} \pm 1.7 \times 10^{-5}$	0.999	5.95×10^{11}

[a] The intercepts and slopes are used in eq 6 (with the Beer–Lambert Law) to yield K_{app} at each pH value.

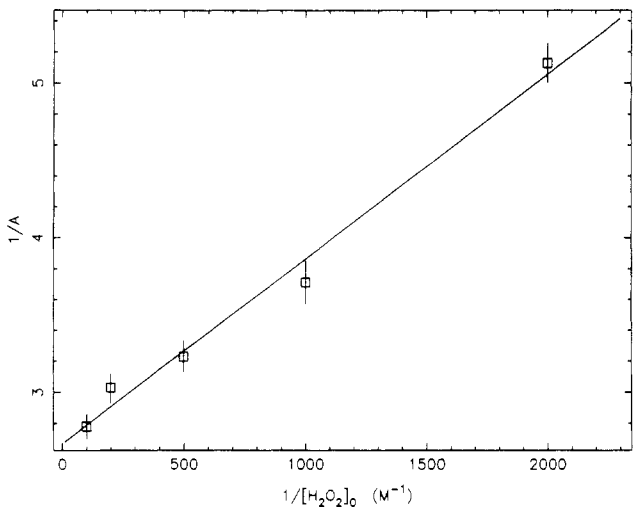

Figure 3. Reciprocal absorbance of the reaction solution vs reciprocal of $[H_2O_2]_0$ (pH 11.4, $[CuSO_4]_0 = 5.0 \times 10^{-5}$ M).

100 times higher than $[Cu^{2+}]_0$) yield the following relation for the concentration of the copper peroxide complex:

$$1/[HO_2\text{–}Cu(I)] = 1/[Cu^{2+}]_0 + \{1 + (K_4 + K_5[OH^-])[OH^-]^3\}/K_{app}[Cu^{2+}]_0[H_2O_2]_0 \quad (6)$$

Since $[HO_2\text{–}Cu(I)] = A/\epsilon L$, where A is the absorbance, ϵ is the extinction coefficient,[13] and L is the path length, plotting $1/A$ vs $1/[H_2O_2]_0$ at constant $[Cu^{2+}]_0$ and $[OH^-]$ will lead to the determination of K_{app}.

Measurements with the pH electrode revealed that the pH increases slowly during the decomposition of H_2O_2 and asymptotically approaches the value corresponding to $[OH^-]_0$ in the absence of H_2O_2. This observation implies that OH^- is not consumed by the reaction; in fact, a small amount of OH^- is actually produced by the decomposition of HO_2^- to oxygen and hydroxide ion. Taking the pH as constant in our analysis does not result in any significant error.

Figure 3 shows a typical plot of reciprocal absorbance vs $1/[H_2O_2]_0$. Linear least-squares fits yield the intercepts and slopes from which K_{app} could be calculated by using eq 6 and literature values of K_4 and K_5. Four determinations were made at pH 11.0, 11.4, 11.7, and 12.0. The results are given in Table II. The choice of this pH range was discussed in the Experimental Section.

K_{app} depends on $[OH^-]$ according to eq 7. Values of K_2 and K_3 obtained by fitting our results to eq 7 by using the known value

$$K_{app} = (K_1K_2[OH^-]^{n+2} + K_3[OH^-]^{n+1})/(1 + K_1[OH^-])$$

or

$$K_1K_2[OH^-] + K_3 = K_{app}(1 + K_1[OH^-])/[OH^-]^{n+1} \quad (7)$$

of K_1 are listed in Table I. Chemically, n can be any integer from 1 to 4, and eq 7 was fit with each of these values. All gave good straight lines, but a positive intercept, i.e., a positive value of K_3, was obtained only with $n = 2$. From this result, the molecular formula of the copper peroxide complex in alkaline media was determined, indirectly, as $HO_2Cu(OH)_2^-$ or $O_2Cu(OH)_2^{2-}$.

Equation 1 implies that K_2 and K_3 are related to the acid/base equilibrium constant of the copper peroxide complex by $K_e = K_1K_2K_w/K_3$, where K_w is the dissociation constant of water. Thus, K_e can be estimated as 3.55×10^{-12} M. Note that only upper limits on K_4 and K_5 are available, which means that the values reported here for K_2, K_3, and K_e are also estimates.

As a check on the validity and consistency of these results, the intercept of eq 6, $1/\epsilon L[Cu^{2+}]_0$ (after applying the Beer–Lambert law), can be used to yield an alternative measurement of the extinction coefficient, ϵ. The calculations were performed with data generated from the linear fits. The numbers ranged from 1480 to 1570 M^{-1} cm^{-1}, in reasonable agreement with our other measurements.

Rate Law and Mechanism. Monitoring the dissolved oxygen concentration at the early stages of its production is a much more sensitive technique than manometric measurement of the gas-phase oxygen pressure, in which processes such as saturation and nucleation can be rate-determining.[5] Therefore, O_2-electrode measurements were used to find the initial rate law.

Figure 4a is a log–log plot showing the dependence of the initial rate on $[H_2O_2]_0$. The initial rate exhibits zero-order dependence when $[H_2O_2]_0/[CuSO_4]_0 > 5$ and first-order dependence when that ratio is $< 1/2$. The initial rate increases at lower $[H_2O_2]_0$ in the right curve (×), since it approaches the point where [Cu(II)] has an effect (see below). Figure 4b shows a strict first-order dependence on $[CuSO_4]_0$ when it is 20-fold less than $[H_2O_2]_0$ but exhibits saturation at higher copper concentrations. This behavior supports the idea that copper(II) serves as a Langmuir-type catalyst rather than as a reaction substrate. Finally, a more interesting dependence on $[NaOH]_0$ is seen in Figure 4c. In a large range, from 3×10^{-5} to 1.6×10^{-2} M, zero-order dependence is observed, followed by an extremely sharp transition to first-order behavior at higher concentrations.

The above results suggest an initial rate law in basic solution of the form

$$(d[O_2]/dt)_0 = A[Cu^{2+}]_0[H_2O_2]_0(D + E[OH^-]_0)/(B + C[H_2O_2]_0) \quad (8)$$

where A, B, C, D, and E are appropriate nonzero parameters, $D \gg E[OH^-]_0$, when $[OH^-]_0 < 1.6 \times 10^{-2}$ M, and $D \approx 0$ when $[NaOH]_0 > 1.6 \times 10^{-2}$ M. Our experiments cannot determine the values of all the coefficients simultaneously.

On the other hand, calculations showed that the curves of log y vs t and $1/y$ vs t shown in Figure 1a,b can be well fit by a function of the form

$$-dy/dt = wy^2/(v + sy + uy^2) \quad (9)$$

where w, v, s, and u are constants whose relationship to the mechanistic parameters of the system will be elucidated below. The first-order term in the denominator was found to have little effect on the shape of the curves in Figure 1 and could even be dropped completely. Plots of reciprocal concentrations vs time (Figure 1b) show a second-order dependence when $[H_2O_2]$ in the system is lower than 10^{-4} M, which is the case when the linear and quadratic terms in the denominator of eq 9 are negligible compared with v.

Assigning $[H_2O_2]$ to y, including $[Cu^{2+}]_0$ in the coefficient w, and fixing $[NaOH]_0 < 10^{-2}$ M make eq 8 consistent with eq 9 ($-2d[H_2O_2]/dt = d[O_2]/dt$) when H_2O_2 is in large excess. The two equations do not agree at low $[H_2O_2]_0$. However, the lowest $[H_2O_2]_0$ in the O_2-electrode experiment data, limited by the experimental conditions, occurs where the $[H_2O_2]$ dependence switches from zeroth to second order (Figure 1a,b). In other words, there is no conflict between the O_2-electrode data and the titration data. Moreover, the O_2-electrode data confirm that the first-order term in the denominator of eq 9 truly exists and

(13) We assume that the protonated and deprotonated forms of the complex, HO_2–Cu(I) and O_2^-–Cu(I), respectively, have similar extinction coefficients.

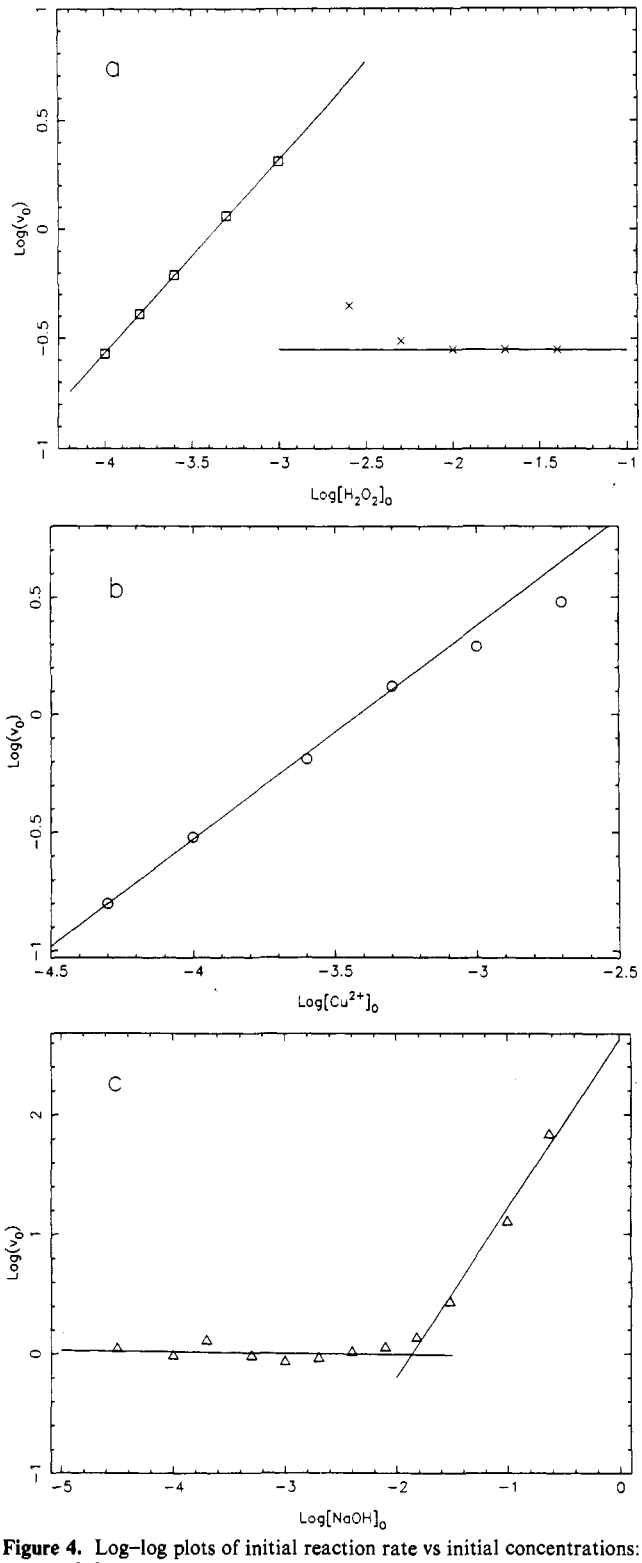

Figure 4. Log–log plots of initial reaction rate vs initial concentrations: (a) $[H_2O_2]_0$; (b) $[CuSO_4]_0$; (c) $[NaOH]_0$. Fixed conditions: (a) $[NaOH]_0 = 8.0 \times 10^{-3}$ M, $[CuSO_4]_0 = 1.0 \times 10^{-4}$ M (×) and 2.0×10^{-3} M (□); (b) $[H_2O_2]_0 = 1.0 \times 10^{-2}$ M, $[NaOH]_0 = 8.0 \times 10^{-3}$ M; (c) $[H_2O_2]_0 = 2.0 \times 10^{-2}$ M, $[CuSO_4]_0 = 1.0 \times 10^{-4}$ M.

dominates for a short interval at the transition from zeroth-order to second-order dependence of the overall rate on $[H_2O_2]$. The second-order dependence of the rate on $[H_2O_2]$ was previously reported for this reaction in acidic media.[14]

Injection of KO_2 into the reaction system, which releases $O_2^{\bullet-}$ radical in aqueous solution instantly,[15] was carried out in the O_2-electrode reactor. Oxygen production was proportional to the amount of KO_2 introduced, but no effect on the reaction rate was observed after the initial spike in $[O_2]$ at the time of injection. This result implies that the $O_2^{\bullet-}$ detected by EPR[8] serves solely as a precursor for molecular oxygen formation but does not react with other intermediates.

Superoxide can appear in both acid and basic forms, $HO_2^{\bullet}$ and $O_2^{\bullet-}$, at the pH's used in this work, since $pK_{HO_2\bullet}$ is 4.75.[16] The kinetics of the disproportionation of superoxide radicals of both forms to give oxygen and hydrogen peroxide have been thoroughly studied and found to obey[16]

$$HO_2^{\bullet} + HO_2^{\bullet} \rightarrow O_2 + H_2O_2 \quad k'$$
$$HO_2^{\bullet} + O_2^{\bullet-} \rightarrow O_2 + HO_2^- \quad k'' \qquad (10)$$
$$O_2^{\bullet-} + O_2^{\bullet-} + H_2O \rightarrow O_2 + HO_2^- + OH^- \quad k^*$$

$$-d[R]/dt = k_{obsd}[R]^2 = k'[HO_2]^2 + k''[HO_2][O_2^{\bullet-}] \qquad (11)$$

where $[R] = [HO_2^{\bullet}] + [O_2^{\bullet-}]$, $K_{HO_2\bullet} = [O_2^{\bullet-}][H^+]/[HO_2^{\bullet}]$, and $k_{obsd} = (k' + k''K_{HO_2\bullet}/[H^+])/(1 + K_{HO_2\bullet}/[H^+])^2$. The above equations were fitted to the experimental data of Bielski and Allen[16] to yield $k' = 7.61 \times 10^5$ M^{-1} s^{-1}, $k'' = 8.86 \times 10^7$ M^{-1} s^{-1}, and $pK_{HO_2\bullet} = 4.75$ and to show that k^* is negligibly small (<0.3 M^{-1} s^{-1}) compared with the other two rate constants. These results are adopted in the analysis that follows.

On the basis of knowledge about the existence and formation of intermediate species, processes found in similar reactions, and the experimental rate law, the five kinetic equations in (12) are proposed to follow the rapid equilibria of eq 2. A suitable

$$O_2Cu(OH)_2^{2-} \rightarrow Cu(OH)_2^- + O_2^{\bullet-} \quad k_6 \text{ (M6)}$$
$$HO_2Cu(OH)_2^- \rightarrow Cu(OH)_2^- + HO_2^{\bullet} \quad k_6' \text{ (M6')}$$
$$Cu(OH)_2^- + O_2 + OH^- \rightarrow Cu(OH)_3^- + O_2^{\bullet-} \quad k_7 \text{ (M7)}$$
$$Cu(OH)_2^- + H_2O_2 \rightarrow Cu(OH)_3^- + OH^{\bullet} \quad k_8 \text{ (M8)}$$
$$Cu(OH)_2^- + HO_2^- + H_2O \rightarrow Cu(OH)_3^- + OH^{\bullet} + OH^- \quad k_8' \text{ (M8')} \qquad (12)$$
$$OH^{\bullet} + H_2O_2 \rightarrow H_2O + HO_2^{\bullet} \quad k_9 \text{ (M9)}$$
$$OH^{\bullet} + HO_2^- \rightarrow H_2O + O_2^{\bullet-} \quad k_9' \text{ (M9')}$$
$$R + R \rightarrow H_2O_2\ (HO_2^-) + O_2\ (+OH^-) \quad k_{10} \text{ (M10)}$$

combination of eq M1–M10 yields the stoichiometry of the disproportionation of H_2O_2 in an alkaline Cu(II) solution, e.g.

$$5Cu^{2+} + 4H_2O_2 + 15OH^- \rightarrow 5Cu(OH)_3^- + 2O_2 + 4H_2O$$

Monomolecular decomposition reactions like (M6) and (M6') are common in transition-state kinetics. Despite the unfavorable potential for reaction M7 in neutral solution, the oxidation of copper(I) by oxygen is well-known, since Cu(I) is not stable in solution or in air. The rate of the reaction varies by several orders of magnitude with different coordinating ligands,[17] and the products should be favored by the strongly alkaline medium. Reaction M8 is analogous to the corresponding reaction in the mechanism of the Fe^{3+}–H_2O_2 system.[2,3] Reaction M9 and its rate constant have been reported by Keyser et al.[18] Reaction M10 is essentially a simplified eq 10, and k_{10} is taken to be the same as k_{obsd}.

The equilibrium concentration of copper peroxide complex is given by eq 13 for the total copper peroxide in the system, where

$$[HO_2\text{–}Cu(I)] = K_{app}[Cu^{2+}]_0[H_2O_2]_f/\{(K_4 + K_5[OH^-])[OH^-]^3 + K_{app}[H_2O_2]_f\} \qquad (13)$$

$[H_2O_2]_f$ is the total free hydrogen peroxide defined in eq 3. The

(14) Sigel, H.; Wyss, K.; Fischer, B. E.; Prijs, B. *Inorg. Chem.* **1979**, *18*, 1354.

(15) Valentine, J. S.; Curtis, A. B. *J. Am. Chem. Soc.* **1975**, *97*, 224.
(16) Bielski, B. H. J.; Allen, A. O. *J. Phys. Chem.* **1977**, *81*, 1048.
(17) Zuberbühler, A. D. In *Copper Coordination Chemistry: Biochemical and Inorganic Perspectives*; Karlin, K. D., Zubieta, J., Eds.; Academic: New York, 1983; p 238 and references therein.
(18) Keyser, L. F.; Choo, K. Y.; Leu, M. T. *Int. J. Chem. Kinet.* **1985**, *17*, 1169.

Table III. Values of the Parameters

$[OH^-]_0$,M	1.0×10^{-3}	3.0×10^{-3}	8.0×10^{-3}
$10^{-5}u/w$	4.61 ± 0.06	3.40 ± 0.05	2.65 ± 0.06
$10^2v/w$	4.6 ± 0.1	4.7 ± 0.2	4.6 ± 0.2
α_1	8.06×10^{-1}	5.81×10^{-1}	3.42×10^{-1}
β_1	7.38×10^{-1}	4.84×10^{-1}	2.60×10^{-1}
q	1.09×10^{-2}	1.47×10^{-2}	1.89×10^{-2}
r	5.13	4.31	4.83

concentrations of the acid and basic forms of the complex may be written in terms of the total copper peroxide as

$$[HO_2Cu(OH)_2^-] = [HO_2\text{–}Cu(I)]/\{1 + (K_e/K_w)[OH^-]\} = \beta_1[H_2O\text{–}Cu(I)] \quad (14)$$

$$[O_2Cu(OH)_2^{2-}] = [HO\text{–}Cu(I)](K_e/K_w)[OH^-]/\{1 + (K_e/K_w)[OH^-]\} = \beta_2[HO_2\text{–}Cu(I)] \quad (15)$$

Using eq 13–15 and applying the steady-state approximation to the species $OH^\bullet$, $HO_2^\bullet$ ($O_2^{\bullet-}$), and $Cu(OH)_2^-$, one obtains the rate law

$$-d[H_2O_2]/dt = 2d[O_2]/dt = 2(\beta_2k_6 + \beta_1k_6') \times (\alpha_1k_8 + \alpha_2k_8')K_{app}[Cu^{2+}]_0[H_2O_2]_f^2/\{k_7[O_2] + (\alpha_1k_8 + \alpha_2k_8')[H_2O_2]_f\}\{(K_4 + K_5[OH^-])[OH^-]^3 + K_{app}[H_2O_2]_f\} \quad (16)$$

in which α_1, α_2, β_1, β_2, and K_{app} are pH-dependent coefficients.

Comparison of eq 16 with eq 9 leads to the following correspondences of the coefficients:

$$w = 2(\beta_2k_6 + \beta_1k_6')(\alpha_1k_8 + \alpha_2k_8')K_{app}[Cu^{2+}]_0$$

$$v = k_7[O_2](K_4 + K_5[OH^-])[OH^-]^3 \quad (17)$$

$$s = k_7[O_2]K_{app} + (\alpha_1k_8 + \alpha_2k_8')(K_4 + K_5[OH^-])[OH^-]^3$$

$$u = (\alpha_1k_8 + \alpha_2k_8')K_{app}$$

Since oxygen bubbles can be seen a few seconds after the reaction starts, the solution is saturated with oxygen almost immediately. Therefore, $[O_2]$ in the solution can be treated as a constant equal to the solubility.

Fitting eq 18, an integrated form of eq 9, to the titrimetric experimental curves shown in Figure 1a,b, should, in principle,

$$t = (v/w)(1/y - 1/y_0) + (s/w)\ln(y_0/y) + (u/w)(y_0 - y) \quad (18)$$

yield the three parameters (v/w, s/w, u/w) in which the unknown rate constants (k_6, k_6', k_7, k_8, k_8') are contained. A nonlinear regression program[19] was employed to carry out this task. However, since there were less than 20 data points in each experimental curve, the three-parameter fits gave standard deviations as large as 50%.

We recall that the qualitative calculation showed the first-order term in the denominator of eq 9 to be of little importance in determining the shape of the integrated y vs t curve. Also, the unknown rate constants in s/w (k_7, k_8, k_8') appear in the other two parameters, v/w and u/w. Therefore, the first-order term was dropped, and two-parameter fits to three sets of experimental data were performed. By this technique, the standard deviations were reduced to less than 4%. The resultant curves of log y or $1/y$ vs time using the fitted parameters are shown with solid lines in Figure 1a,b.

The purpose of the above procedure is to generate approximate values of the unknown rate constants through the fitted parameters (eq 17). Rearranging eq 17 as eq 19 and 20 and using the

$$(k_6' + k_6)\beta_1 + k_6 = 1/\{2(u/w)[Cu^{2+}]_0\} = q \quad (19)$$

$$(k_8/k_7 - k_8'/k_7)\alpha_1 + k_8'/k_7 = (u/v)[O_2](K_4 + K_5[OH^-])[OH^-]^3/K_{app} = r \quad (20)$$

parameter values listed in Table III, we can calculate the desired results from the slopes and intercepts of the straight lines q vs β_1 and r vs α_1.

Equation 19 was used to fit the data, from which k_6 and k_6' were estimated as 2.3×10^{-2} s^{-1} and 6.3×10^{-3} s^{-1}, respectively. Results from this three-point fit are crude, but fortunately only the approximate values of these rate constants are of interest here. All of the values were then optimized in the computer simulations described below. The fit of eq 20 at three different $[OH^-]$ values did not give a good straight line but could be viewed as a line of zero slope with a large deviation. Since we are interested only in rough estimates of the rate constants, we took $k_8' = k_8$. Thereafter, the ratio k_8/k_7 was obtained as the average of r, 4.76 M. However, the individual values of k_8 and k_7 could not be deduced at this stage.

Computer Simulations. Applying the law of mass action to eq 12 yields the following rate and differential equations for the nonequilibrium chemical species:

$$v(1) = \beta_2k_6[HO_2\text{–}Cu(I)]$$

$$v(2) = \beta_1k_6'[HO_2\text{–}Cu(I)]$$

$$v(3) = 10^{-3}k_7[Cu(OH)_2^-] \quad (21)$$

$$v(4) = k_8[Cu(OH)_2^-][H_2O_2]_f$$

$$v(5) = k_9[OH^\bullet][H_2O_2]_f$$

$$v(6) = k_{10}[R]^2$$

$$d[H_2O_2]_f/dt = -v(1) - v(2) - v(4) - v(5) + v(6)$$

$$d[Cu(OH)_2^-]/dt = v(1) + v(2) - v(3) - v(4)$$

$$d[R]/dt = v(1) + v(2) + v(3) + v(5) - 2v(6) \quad (22)$$

$$d[OH^\bullet]/dt = v(4) - v(5)$$

$$d[O_2]/dt = -v(3) + v(6)$$

where the equilibrium concentrations of the copper peroxide complexes are expressed by eq 13–15.

Integration of the differential equations (22) gives the concentrations of the relevant chemical species as functions of time. The Gear numerical integrator[20] was used. At each call to the integrator subroutine, the equilibrium concentration of HO_2–Cu(I) complex was recalculated before being introduced into the kinetic processes with $[H_2O_2]_f$ obtained from the last integration step. $[OH^-]$ was treated as a constant. The three pH values used in the titrimetric experiments were used in the simulation to generate curves of $[H_2O_2]$ vs time. Rate constants k_9 and k_{10} were taken from the literature, while k_6, k_6', k_7, and k_8 were optimized to give the best fit to the experimental data. The results are plotted in Figure 5, in which excellent agreement can be seen in all three curves so long as $[H_2O_2]$ remains higher than 10^{-4} M. Since, in the experiments, acidification causes equilibria M2 and M3 to shift to the left, releasing hydrogen peroxide, and this amount is then titrated by $KMnO_4$, $[H_2O_2]_f + [HO_2\text{–}Cu(I)]$ was plotted vs time for greater accuracy. However, there was no observable effect of including $[HO_2\text{–}Cu(I)]$ when $[H_2O_2]_f > 10^{-4}$ M, since the total concentration of copper is less than 10^{-4} M.

The optimized rate constants are listed in Table I. Rate constants k_6 and k_6' were found to be close to the results from the nonlinear regression, while the ratio k_8/k_7 was shifted from 4.76 to 16.7 M. This ratio is critical in determining the shape of the curve at $[H_2O_2] < 10^{-4}$ M but has little effect on the behavior at higher peroxide concentrations. The individual values for k_7 and k_8 can range from a minimum of about 50 M^{-2} s^{-1} for k_8 to values as much as 9 orders of magnitude higher without affecting the results, as long as the ratio is held fixed. The lower limit for k_8 corresponds to the value at which $v(7) + v(8) \approx v(6) + v(6')$; above this value, reactions M7 and M8 proceed more rapidly than reactions M6 and M6′. These observations strongly suggest that

(19) PAR, written by: Ralston, M. In *BMDP Statistical Software*; Dixon, W. J., Ed.; University of California Press: Berkeley, CA, 1983.

(20) Gear, C. W. *Numerical Initial Value Problems in Ordinary Differential Equations*: Prentice-Hall: Englewood Cliffs, NJ, 1971.

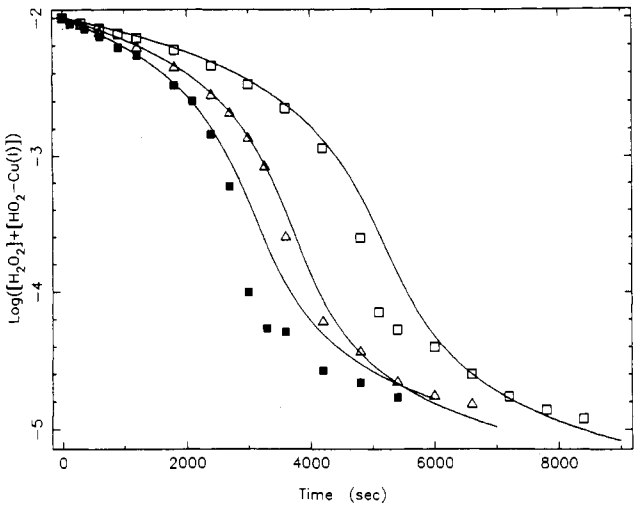

Figure 5. Integrated $[H_2O_2]$ vs time calculated by using the mechanism (M1)–(M10) and the constants listed in Table I (all solid lines). Symbols for experimental data and initial conditions are as in Figure 1.

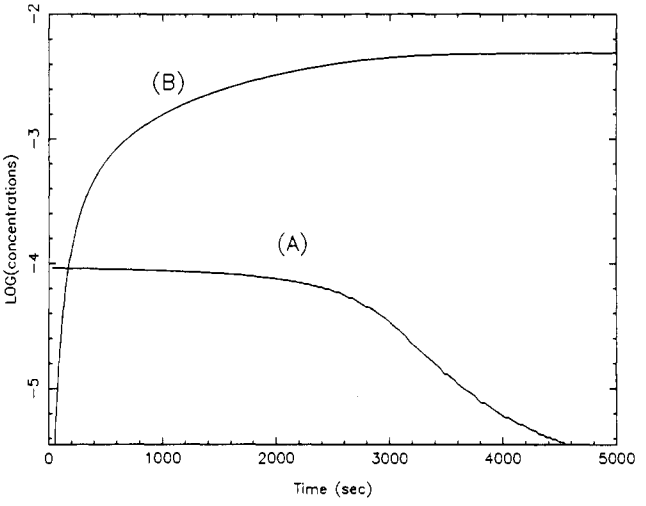

Figure 6. Calculated concentrations of (A) copper–peroxide complex and (B) molecular oxygen evolved determined by using the mechanism (M1)–(M10) and the constants listed in Table I ($[NaOH]_0 = 8.0 \times 10^{-3}$ M, $[H_2O_2]_0 = 1.0 \times 10^{-2}$ M, $[CuSO_4]_0 = 1.0 \times 10^{-4}$ M).

reactions M6 and M6′ rather than reactions M7 and M8 (or M8′) are rate-determining for the radical formation process. The rates of reactions M7 and M8 are limited in any case by the amount of Cu(I) supplied by reaction M6 (or M6′), and the fast radical-consuming steps that follow will maintain the radicals in a steady state. Thus, so long as k_7 and k_8 are large enough so that (M7) and (M8) are not rate-determining, one should not expect the kinetic behavior of the system to be sensitive to their actual values.

One source of the systematic discrepancy between the experimental and theoretical curves when $[H_2O_2] < 10^{-4}$ M (Figure 5) is obvious: $[OH^-]$ was treated, for simplicity, as a constant throughout the reaction. Actually, eq M1 shows that H_2O_2 is an acid. As H_2O_2 is consumed, if there is no step that removes OH^-, the concentration of OH^- should build up. The pH-electrode experiment verifies this prediction. Since higher $[OH^-]$ increases the rate of the reaction, i.e., shifts the $[H_2O_2]$ vs time curve to the left, a better match of the calculation with the titration curve can be expected if the increase in $[OH^-]$ is taken into account.

As additional support for the mechanism, Figure 6 gives plots of the calculated O_2 evolution and $[HO_2–Cu(I)]$ vs time. The simulations reproduce the major features of the experimental curves in Figures 2 and 7. The concentration of the copper peroxide complex remains constant at its maximum until the H_2O_2 concentration drops below 10^{-4} M. Oxygen is released instantly when the reagents are mixed, but its rate of production slows significantly by the time 90% of the H_2O_2 has decomposed.

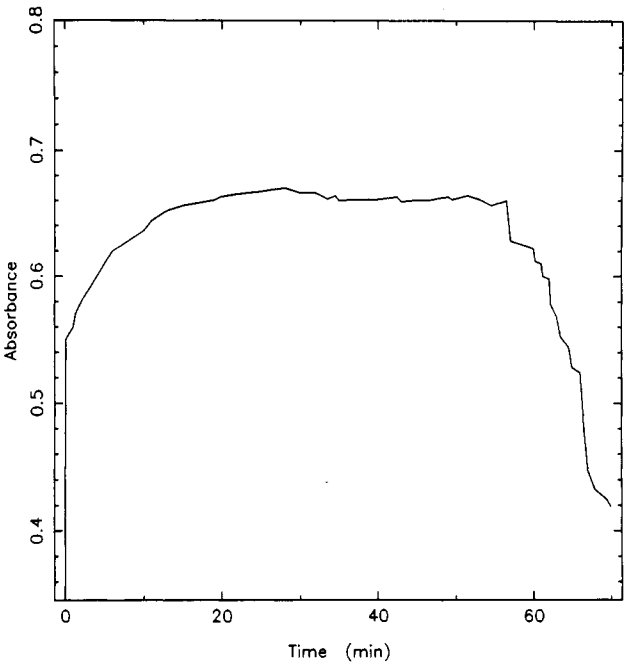

Figure 7. Optical absorbance vs time ($\lambda = 370$ nm, $[H_2O_2]_0 = 1.0 \times 10^{-2}$ M, $[CuSO_4]_0 = 1.0 \times 10^{-4}$ M, $[NaOH]_0 = 8.0 \times 10^{-3}$ M).

Discussion

We have proposed a molecular formula for the complex postulated to serve as the precursor in the copper(II)-catalyzed decomposition of H_2O_2 in basic solution. The apparent formation constant has been measured as a function of pH in the range 11–12. We emphasize that the dependence of the apparent formation constant on $[OH^-]$ found here is strictly valid only in that pH range. The distribution diagram of copper(II) hydroxides[12] shows that other species not considered here become significant at higher or lower pH's. For example, only $Cu(OH)_4^{-2}$ is significant at pH >12, while $Cu_2(OH)_2^{2+}$ becomes dominant in the pH range 8–10. Thus, the apparent formation constant directly derived from the simultaneous equilibria in the system should have a different dependence on $[OH^-]$ in different pH ranges. Even the formula of the complex (more accurately, the number of associated hydroxide anions) may vary with pH. More measurements need to be done with other methods for the molecular formula and the apparent formation constants to span a wider pH range.

The validity of the mechanism proposed here is limited to pH <12. The sharp rise in the initial reaction rate at higher pH depicted in Figure 4c clearly demonstrates that some more rapid reactions omitted from our mechanism must be taken into account under those conditions. It is likely that other, more reactive species will need to be invoked, but we have not attempted to analyze the high-pH regime further in the present study.

We have accounted for the Cu(II) EPR silence of the proposed $Cu(II)–H_2O_2$ complex by postulating that electron transfer is nearly instantaneous and that Cu(II) is reduced to Cu(I) before the complex dissociates. This assumption is supported by the estimated extinction coefficient, which is typical of an electron-transfer complex. To indicate this view more clearly, we have denoted the complex as $HO_2–Cu(I)$ so that the oxidation state of copper is pointed out explicitly; i.e., we view the complex as EPR-silent Cu(I) in coordination with superoxide. By "EPR-silent", we mean that there is no copper signal, though there may be unpaired spin density on the superoxide, with a frequency different from that of copper. The EPR experiment does indeed show a strong superoxide signal both in the precipitated complex and in solution. Unfortunately, an EPR experiment on a solution with our experimental composition would probably not be conclusive, since the kinetic balance between Cu(I) and Cu(II) is established rapidly and is maintained throughout the reaction.

A brown precipitate was observed in several studies[4,9,11] with higher $[Cu^{2+}]_0$ in alkaline H_2O_2. In dilute solution, the negative charge of the HO_2–Cu(I) complex can keep it dissolved. We suggest that the precipitate that occurs at higher concentrations has the "molecular" formula of the ring-structured dimer shown as follows:

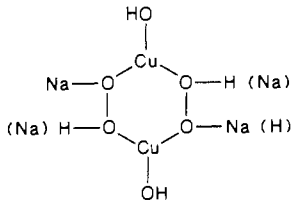

Sigel et al.,[6] in a mechanistic study of this reaction in acidic medium, also propose a ring-structured copper peroxide complex as an intermediate in which the copper cation remains in the original oxidation state while two molecules of hydrogen peroxide disproportionate through the ring frame. The d-orbital complex feature of that $(H_2O_2)_2$–Cu(II) complex is consistent with its lack of color. The drastic slowing down of the acidic H_2O_2 decomposition compared with that in basic solution probably results from the extensive steric requirements of all the associated atoms in the complex, with Cu(II) serving as nothing more than a connector for the two reacting H_2O_2 molecules. The transition from the electron-transfer complex to the d orbital is manifested as a sharp color change when the pH of the system is adjusted as described in the Experimental Section.

The most important influence on the alternation of reaction pathway and, consequently, on the dramatic change in reaction rate in going from acidic to alkaline conditions is probably the pH dependence of the redox potential of the couple $HO_2^{\bullet}$ $(O_2^{\bullet-})/H_2O_2$ (HO_2^-).[21] The redox potential drops from 1.4 to 0.18 V over the pH range 0–14. It is obvious that the oxidation of H_2O_2 to $HO_2^{\bullet}$ or $O_2^{\bullet-}$ by metal ions such as Cu^{2+} and Fe^{3+} is highly unfavorable in an acidic medium but possible in an alkaline environment.

Two completely different mechanisms for Fe^{3+}-catalyzed H_2O_2 decomposition have been debated since the 1950s.[7] They are the "free-radical" mechanism proposed by Haber and Weiss[2] and reinvestigated by Barb et al.[3] and the "complex" mechanism developed by Kremer and Stein.[4] Experimental evidence has been obtained both for the existence of $OH^{\bullet}$ and $HO_2^{\bullet}$ radicals and for the formation of a Fe^{3+}–HO_2^- complex. Both mechanisms are successful to some extent, but both have limitations, discussed in detail in a recent review.[7] Unimolecular decomposition of a ferric peroxide complex was one of the key features of the "complex" mechanism. To avoid invoking radicals, the complex is assumed to decompose to another complex, FeO^{3+}, which is less convincingly proved, rather than to a state in which the radical and the reduced metal ion are separated. The latter assumption would lead to a unified mechanism to account for the fact that Fe^{2+} can initiate the catalysis as well as sustain it.[3] We suggest that combination of the two mechanisms, much as has been done in this work, may provide an improved mechanism for Fe^{3+}-catalyzed H_2O_2 decomposition.

However, the much lower redox potential of the Cu^{2+}/Cu^+ couple compared with those of Fe^{3+}/Fe^{2+}, Co^{3+}/Co^{2+}, etc. makes it different from those metal catalysts. The generation of a chemical oscillator with H_2O_2 and KSCN[22] is a consequence of that difference. In fact, this work was initially motivated by the attempt to understand the oscillatory system. With better knowledge of the Cu^{2+} reaction with H_2O_2, progress is being made toward that goal.

Acknowledgment. Prof. Miklós Orbán is sincerely acknowledged for helpful information and discussions. Y.L. thanks Prof. W. Phil Huskey for help in using some of the computer programs and Eric S. Furfine for assistance in using the O_2-electrode device. This work was supported by the National Science Foundation (Grant No. CHE-8419949).

Registry No. H_2O_2, 7722-84-1; Cu, 7440-50-8; $HO_2Cu(OH)_2^-$, 114720-37-5.

(21) Fee, J. A.; Valentine, J. S. In *Superoxide and Superoxide Dismutases*; Michelson, A. M., McCord, J. M., Fridovich, I., Eds.; Academic: New York, 1977; p 28.

(22) Orbán, M. *J. Am. Chem. Soc.* **1986**, *108*, 6893.

Contribution from the Department of Inorganic Chemistry, University of Sydney, Sydney, NSW 2006, Australia

Steric Contributions to the Thermodynamics of Electron Transfer in Cobalt(III) Hexaamine Complexes

Trevor W. Hambley

Received December 1, 1987

Molecular mechanics modeling of the Co(III) and Co(II) oxidation states for a number of complexes with six saturated amine donor atoms shows that differences in the change in strain energy on reduction of Co(III) result from the different abilities of ligands to accommodate the change in bond lengths that occurs concomitant with reduction. This change in strain energy correlates closely with the Co(III)/Co(II) reduction potential. Differences in strain energy changes on reduction contribute up to 96 kJ mol^{-1} (1 V) to the differences in reduction potentials. Thus, steric relaxation contributes significantly to the thermodynamics of electron transfer and needs to be taken into account when reduction potentials of Co(III) complexes are compared. Analysis of the reduction potentials with the steric relaxation contribution removed reveals an empirical correlation with either the degree of substitution at the amine nitrogen or the number of amine hydrogen atoms and suggests that the reduction potential may be dependent on the Lewis basicity of the ligand. A correlation also exists between the strain energy relaxation that occurs on lengthening the Co–N bond and the frequency of the low-energy d–d transition in Co(III) complexes suggesting that this transition is also accompanied by a lengthening of the Co–N bond and that there is a steric contribution to the ligand field strength.

Introduction

The recent report of a Co(III)/Co(II) reduction potential of –0.63 V (vs NHE) for the macrocyclic complex $[Co(diammac)]^{3+}$ (diammac = 6,13-diamino-6,13-dimethyl-1,4,8,11-tetraazacyclotetradecane, Chart I), when taken with the value of 0.28 V for $[Co(dpt)_2]^{3+}$ [dpt = bis(3-aminopropyl)amine],[2] means that reported reduction potentials for cobalt(III) hexaamine complexes range over more than 0.9 V. Given that these complexes have identical first coordination spheres (i.e. six amine nitrogen donor atoms), the question arises as to what causes such a wide range

(1) Curtis, N. F.; Gainsford, G. J.; Hambley, T. W.; Lawrance, G. A.; Morgan, K. R.; Siriwardena, A. *J. Chem. Soc., Chem. Commun.* **1987**, 295–7.

(2) Wieghardt, K.; Schmidt, W.; Herrmann, W.; Kippers, H.-J. *Inorg. Chem.* **1983**, *22*, 2953–6.

0020-1669/88/1327-2496$01.50/0